

Bulk Weak Ferromagnet in Ferrimagnetic Chains of Organic–Inorganic Hybrid Materials Based on BDH-TTP and Paramagnetic Thiocyanato Complex Anions: (BDH-TTP)[M(isoq)₂(NCS)₄], M = Cr^{III}, Fe^{III}

Fatima Setifi,[†] Stéphane Golhen,[†] Lahcène Ouahab,^{*†} Akira Miyazaki,^{*‡} Kazuki Okabe,[‡] Toshiaki Enoki,^{*‡} Takashi Toita,[§] and Jun-ichi Yamada^{*§}

LCSIM, UMR 6511 CNRS, Université de Rennes I, Institut de Chimie de Rennes, 35042 Rennes Cedex, France, Department of Chemistry, Graduate School of Science and Engineering, Tokyo Institute of Technology, Ookayama, Meguro-ku, Tokyo 152-8551, Japan, and Department of Material Science, Faculty of Science, Himeji Institute of Technology, 3-2-1 Kouto, Kamigori-cho Ako-gun, Hyogo 678-1297, Japan

Received February 21, 2002

The preparation, X-ray crystal structures, and magnetic properties of two new isostructural charge transfer salts, (BDH-TTP)M(isoq)₂(NCS)₄ (M = Cr^{III} (1), Fe^{III} (2), BDH-TTP = 2,5-bis(1,3-dithiolan-2-ylidene)-1,3,4,6-tetrathiapentalene, isoq = isoquinoline), are reported. Crystal data for 1: monoclinic, space group *C2/c* (#15), *a* = 16.1363(9) Å, *b* = 19.0874(12) Å, *c* = 12.5075(6) Å, β = 95.70(4)°, *V* = 3833.2(4) Å³, *Z* = 4, *R* = 0.0516 for 2844 reflections with *I* > 2σ(*I*); for 2: monoclinic, *C2/c* (#15), *a* = 16.1938(8) Å, *b* = 19.1117(11) Å, *c* = 12.5100(10) Å, β = 94.265(3)°, *V* = 3861.0(4) Å³, *Z* = 4, *R* = 0.0479 for 2969 reflections with *I* > 2σ(*I*). The crystal structure consists of zigzag mixed organic and inorganic layers, and each layer is formed by mixed columns of BDH-TTP radical cations and paramagnetic metal complex anions. Short intermolecular atomic contacts between donor and anion are observed within the column in the *c*-direction. The two compounds have weak room-temperature electrical conductivities. ESR measurements show a single signal without separating the donor and anion spins, suggesting a π interaction between the d and π electrons. For both compounds ferrimagnetic interactions are observed between the nonequivalent donor and anion spins. These materials exhibit bulk canted weak ferromagnetism below 7.6 K for both 1 and 2.

Introduction

Great interest is currently devoted to organic/inorganic hybrid molecular materials combining conducting electrons and localized spins.^{1–5} The aim is to obtain a long-range magnetic coupling between isolated localized spins of the inorganic networks containing transition metals (d electrons)

through the mobile electrons of the organic networks (π electrons). To establish a magnetic interaction between these two parts, structural interactions between them are essential. Recently Day and co-workers reported that salts of TTF (tetrathiafulvalene) and its derivative with [Cr(NCS)₄(L)_{*n*}][–] (L = 1,10-phenanthroline or isoquinoline (see below)) show bulk ferrimagnetism.⁶ These salts were designed with the idea that magnetic interactions would be induced by both

* Corresponding authors. E-mail: ouahab@univ-rennes1.fr (L.O.); tenoki@chem.titech.ac.jp (T.E.); miyazaki@chem.titech.ac.jp (A.M.); yamada@sci.himeji-tech.ac.jp (J.Y.).

[†] Université de Rennes I.

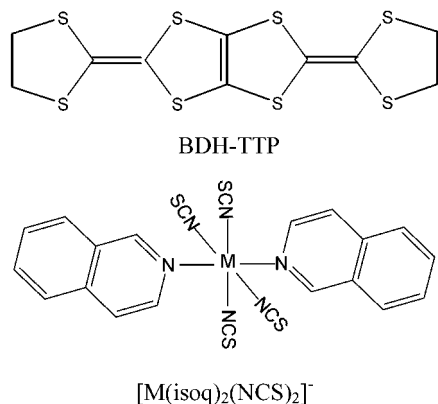
[‡] Tokyo Institute of Technology.

[§] Himeji Institute of Technology.

- (1) (a) Day, P.; Kurmoo, M.; Mallah, T.; Marsden, I. R.; Friend, R. H.; Pratt, F. L.; Hayes, W.; Chasseau, D.; Gaultier, J.; Bravic, G.; Ducasse, L. *J. Am. Chem. Soc.* **1992**, *114*, 10722. (b) Graham, A. W.; Kurmoo, M.; Day, P. *J. Chem. Soc., Chem. Commun.* **1995**, 2061. (c) Kobayashi, H.; Tomita, H.; Naito, T.; Kobayashi, A.; Sakai, F.; Watanabe, T.; Cassoux, P. *J. Am. Chem. Soc.* **1996**, *118*, 368. (d) Kobayashi, H.; Kobayashi, A.; Cassoux, P. *Chem. Soc. Rev.* **2000**, *29*, 325.
- (2) Le Maguerès, P.; Ouahab, L.; Conan, N.; Gomez-Garcia, C. J.; Delhaès, P.; Even, J.; Bertault, M. *Solid State Commun.* **1996**, *97/1*.

- (3) (a) Nishijo, J.; Ogura, E.; Yamaura, J. I.; Miyazaki, A.; Enoki, T.; Takano, T.; Kuwatani, Y.; Iyoda, M. *Solid State Commun.* **2000**, *116*, 661. (b) Thoyon, D.; Okabe, K.; Imakubo, T.; Golhen, S.; Miyazaki, A.; Enoki, T.; Ouahab, L. *Mol. Cryst. Liq. Cryst.* **2002**, *376*, 25.
- (4) Ouahab, L. *Chem. Mater.* **1997**, *9*, 1909.
- (5) Coronado, E.; Galan-Mascaros, J. R.; Gomez-García, C. J.; Laukhin, V. N. *Nature* **2000**, *408*, 447.
- (6) (a) Turner, S. S.; Michaut, C.; Durot, S.; Day, P.; Gelbrich, T.; Hursthouse, M. B. *J. Chem. Soc., Dalton Trans.* **2000**, 905. (b) Turner, S. S.; Le Pevelen, D.; Day, P.; Prout, K. *J. Chem. Soc., Dalton Trans.* **2000**, 2739. (c) Setifi, F.; Golhen, S.; Ouahab, L.; Turner, S. S.; Day, P. *Cryst. Eng. Commun.* **2002**, *4*, 1.

S...S contacts and π - π stacking overlap between the magnetic anions and organic radicals. Indeed a large number of the salts showed long-range ferrimagnetic order with T_C 's ranging from 4.2 to 8.9 K. Other work, in this area, is based on interactions through $-N\cdots I-$ contacts³ or coordinate bonding⁷ between the conducting and the paramagnetic networks. Up to now, investigations are oriented toward salts based on TTF derivatives, which exhibit a wide variety of electronic characteristics, such as semiconductors, metals, and superconductors, depending on the counteranion.⁸ Recently BDH-TTP (2,5-bis(1,3-dithiolan-2-ylidene)-1,3,4,6-tetrathiapentalene)⁹ (see below), which does not have a TTF moiety, is found to produce salts showing metallic state down to low temperatures regardless of the counteranions. There is, therefore, keen interest in studying BDH-TTP salts containing paramagnetic anions in the development of new organic/inorganic hybrid molecular materials. Here we report the preparation, crystal structures, and magnetic properties of (BDH-TTP)[M(isoq)₂(NCS)₄] (M = Cr^{III}, Fe^{III} and isoq = isoquinoline).



Experimental Section

Synthesis. All experiments were conducted under nitrogen or argon. The solvents were distilled before use, and the starting reagents were used as received. Black crystals of compounds **1** and **2** were obtained on a platinum electrode by anodic oxidation of the donor BDH-TTP⁹ (8 mg) under argon atmosphere, using (isoqH)[Cr(isoq)₂(NCS)₄]·3H₂O or (Bu₄N)[Fe(isoq)₂(NCS)₄]⁶ (100 mg) in CH₂Cl₂ (20 mL) as electrolyte. The crystal growth apparatus for electrocrystallization consists of a glass U-cell with two compartments (10 mL each) separated by a glass frit and two platinum wire electrodes (diameter = 1 mm). A low constant current of $I = 1 \mu\text{A}$ was applied and maintained during two weeks.

Crystallographic Data Collection and Structure Determination. Single crystals of the title compounds (**1** and **2**) were mounted on a Nonius four-circle diffractometer equipped with a CCD camera and a graphite-monochromated Mo K α radiation source ($\lambda = 0.71073 \text{ \AA}$). Effective absorption correction was performed (SCALEPACK¹⁰). Structures were solved with direct methods and

Table 1. Crystal Data and Structure Refinement for **1** and **2**

	1	2
empirical formula	C ₃₂ H ₂₂ CrN ₆ S ₁₂	C ₃₂ H ₂₂ FeN ₆ S ₁₂
fw	927.28	931.13
temp/K	120(2)	120(2)
radiation, $\lambda/\text{\AA}$	0.71073	0.71073
cryst syst	monoclinic	monoclinic
space group	C2/c (# 15)	C2/c (# 15)
a/ \AA	16.1363(9)	16.1938(8)
b/ \AA	19.0874(12)	19.1117(11)
c/ \AA	12.5075(6)	12.5100(10)
α/deg	90.	90.
β/deg	95.70(4)	94.265(3)
γ/deg	90.	90.
V/ \AA^3	3833.3(4)	3861.0(4)
Z	4	4
$d_{\text{calc}}/\text{g}\cdot\text{cm}^{-3}$	1.607	1.602
μ/mm^{-1}	0.987	1.075
no. of reflns collected	7847	8548
no. of ind reflns	4358	4426
[$I > 2\sigma(I)$]	2844	2967
final R1, ^a wR2 ^b	0.0516, 0.1185	0.0479, 0.1134

$$^a R1 = \frac{\sum ||F_o| - |F_c||}{\sum |F_o|}, \quad ^b wR2 = \left\{ \frac{\sum [w(F_o^2 - F_c^2)^2]}{\sum [w(F_o^2)^2]} \right\}^{1/2}.$$

refined with the full matrix least-squares method on F^2 using SHELX-97¹¹ programs. In compound **2**, a disorder is observed for one of the two terminal ethylenic carbon atoms of BDH-TTP, which is shifted on two positions (C15A and C15B). Crystallographic data are summarized in Table 1. Full bond lengths and bond angles, atomic coordinates, and complete crystal structure results are deposited as Supporting Information.

Physical Property Measurements. Magnetic susceptibilities were measured using a Quantum Design MPMS-5 SQUID magnetometer down to 1.8 K with an applied field of 10 mT using nonoriented microcrystalline samples in aluminum foil. For compound **1**, measurements on aligned single crystalline samples are also performed. ESR spectra for the nonoriented microcrystalline samples were recorded with a JEOL TE-200 spectrometer equipped with an Oxford ESR910 cryostat.

Results and Discussion

Crystal Structures. Selected bond distances and bond angles are given in Table 2. ORTEP drawings of the molecular structure for **1** with the atomic numbering scheme is shown in Figure 1a.

Since the two compounds are isostructural, we describe here the structure of compound **1** and we give the data for compound **2** in square brackets. An asymmetric unit contains half of an anion and half of a BDH-TTP molecule, both lying on inversion centers in special positions, (1/4, 1/4, 0) and (1/4, 1/4, 1/2), respectively. The M-N (of NCS) distances (average value 1.991(3) [2.028(4)] \AA) are slightly shorter than those to isoquinoline (M-N3 = 2.078(3) [2.160(3)] \AA); hence the MN₆ coordination octahedra are axially distorted. From the 1:1 stoichiometry, the charge on the donor molecule is assumed equal ca. +1. As shown in Figure 1b, in the crystal structure the cations and anions form mixed zigzag layers within the bc -plane, which are then stacked along the

(7) Iwahori, F.; Golhen, S.; Ouahab, L.; Carlier, R.; Sutter, J. P. *Inorg. Chem.* **2001**, *40*, 6541.

(8) Williams, J. M.; Ferraro, J. R.; Thorn, R. J.; Carlson, K. D.; Geiser, U.; Wang, H. H.; Kini, A. M.; Whangbo, M. H. In *Organic Superconductors. Synthesis, Structure, Properties and Theory*; Grimes, R. N., Ed.; Prentice Hall: Englewood Cliffs, NJ, 1992.

(9) Yamada, J.; Watanabe, M.; Anzai, H.; Nishikawa, H.; Ikemoto, I.; Kikuchi, K. *Angew. Chem., Int. Ed.* **1999**, *38*, 810.

(10) Otwinowski, Z.; Minor, W. Processing of X-ray Diffraction Data Collected in Oscillation Mode. In *Methods in Enzymology*; Carter, C. W., Jr., Sweet, R. M., Eds.; Academic Press: New York, 1997; Vol. 276: Macromolecular Crystallography, part A, pp 307-326.

(11) Sheldrick, G. M. *SHELX 97, Program for the Refinement of Crystal Structures*; University of Göttingen: Germany, 1997.

Table 2. Bond Lengths (Å) and Angles (deg) for **1** and **2**

	1	2
M–N(1)	1.991(3)	2.037(3)
M–N(2)	1.991(3)	2.025(3)
M–N(3)	2.078(3)	2.160(3)
S(4)–C(12)	1.712(4)	1.724(4)
S(4) ⁱ –C(13)	1.746(4)	1.751(4)
S(3)–C(12)	1.726(4)	1.726(4)
S(3)–C(13)	1.729(4)	1.743(4)
S(5)–C(14)	1.718(4)	1.734(4)
S(5)–C(15)	1.755(7)	S(5)–C(15A) 1.732(11)
		S(5)–C(15B) 1.842(1)
S(6)–C(14)	1.743(5)	1.743(4)
S(6)–C(16)	1.798(4)	1.809(4)
C(1)–S(1)	1.628(4)	1.623(4)
C(2)–S(2)	1.630(4)	1.614(4)
C(12)–C(12) ⁱ	1.370(8)	1.375(7)
N(1)–M–N(2)	90.43(14)	89.41(12)
N(1)–M–N(3)	90.14(13)	90.54(11)
N(2)–M–N(3)	89.42(13)	89.55(11)
C(12)–S(3)–C(13)	94.1(2)	94.16(17)
C(12)–S(4)–C(13) ⁱ	94.19(19)	93.67(17)
C(14)–S(5)–C(15)	95.5(3)	C(14)–S(5)–C(15A) 93.6(4)
		C(14)–S(5)–C(15B) 95.16(13)
C(14)–S(6)–C(16)	96.2(2)	95.51(18)
C(1)–N(1)–M	175.9(3)	176.5(3)
C(2)–N(2)–M	171.7(3)	170.0(3)

i: $-x + 1/2, -y + 1/2, -z + 1$.

b-direction. The layer consists of one-dimensional chains elongated in the *c*-direction (Figure 2). The S⋯S distances of the short intermolecular contacts within the chain (S2–S3, 3.264(2) [3.286(1)]; S2–S4, 3.397(2) [3.400(2)]; S1–S5, 3.365(2) [3.423(1)] Å) are remarkably shorter than the van der Waals distance (3.70 Å).¹² The adjacent chains are then connected with a π – π overlap of isoquinoline moieties (interplanar separation: $d = 3.600(5)$ [3.582(5)] Å) between the anions and a short S⋯S contact (S5–S5 = 3.640(2) [3.638(2)] Å, not shown in Figure 2) between the donors. In the [101] direction, the neighboring anions are related by the *c*-glide plane, and therefore the orientation of these anions is different; the angle between the molecular axes (defined as isoq–M–isoq axes) is 6.0(3)° [3.5(2)°]. The difference in the orientation of the units in the [101] direction can be seen more clearly considering the BDH-TTP donors which are orthogonal to each other.

Physical Properties. The salts have low conductivity ($\sigma(300\text{ K}) = 10^{-5}\text{ S cm}^{-1}$) due to the 1:1 stoichiometry and the alternate stacking of donors and anions. The temperature dependences of $\chi_M T$ and χ_M^{-1} at 10 mT, where χ_M is the molar magnetic susceptibility for the nonoriented microcrystalline sample, after subtracting core diamagnetism contribution are shown in Figure 3a and 3b for compounds **1** and **2**, respectively. Due to the isomorphous nature of these two salts, their magnetic properties show similar behaviors. The susceptibility obeys the Curie–Weiss law above 50 K. The Curie constant *C* and Weiss temperature Θ are estimated as $C = 2.19\text{ emu K mol}^{-1}$, $\Theta = -20.4\text{ K}$ for **1**, and $C = 4.95\text{ emu K mol}^{-1}$, $\Theta = -10.1\text{ K}$ for **2**. These Curie constants are close to the corresponding spin-only value (2.25 emu K mol⁻¹ for **1**, 4.75 emu K mol⁻¹ for **2**) for noninteracting anion ($S = 3/2$ for **1**, $5/2$ for **2**) and donor ($S = 1/2$)

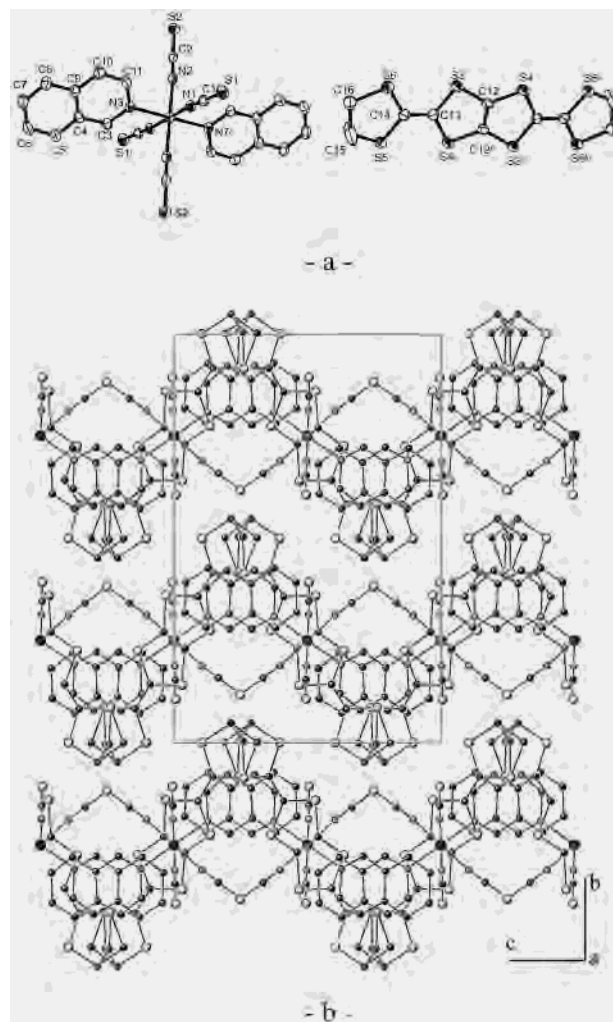


Figure 1. (a) ORTEP diagram with 50% probability level and atom-numbering scheme for **1**. (b) Projection of the crystal structure onto the *bc*-plane, showing the π overlap between the isoquinoline ligands and the BDH-TTP molecules.

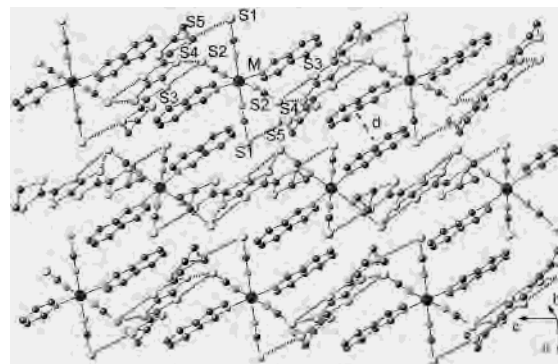
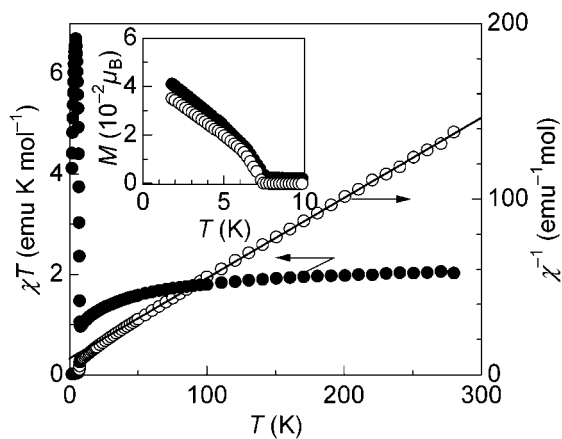


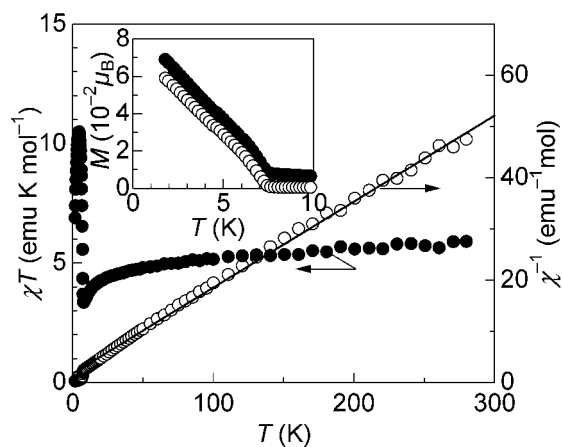
Figure 2. Projection of the mixed layer onto the *ac*-plane showing the mixed chain of anion and donor; dotted lines indicate the anion–anion overlap (interplanar separation: $d = 3.600(5)$ [3.582(5)] Å) and intermolecular S⋯S contacts (S2⋯S3: 3.264(2) [3.286(1)], S2⋯S4: 3.397(2) [3.400(2)], S1⋯S5: 3.365(2) [3.423(1)] Å).

spins, assuming $g = 2.0$ for each species. Below 50 K $\chi_M T$ decreases as the temperature decreases down to 8 K, showing the antiferromagnetic coupling between the anion and donor spins. For both salts, $\chi_M T$ shows a steep increase at $T_C = 7.6\text{ K}$ due to a magnetic transition. The insets of Figure 3a and 3b present the field-cooled magnetization (FCM) mea-

(12) Bondi, A. *J. Phys. Chem.* **1964**, *68*, 441.



(a)

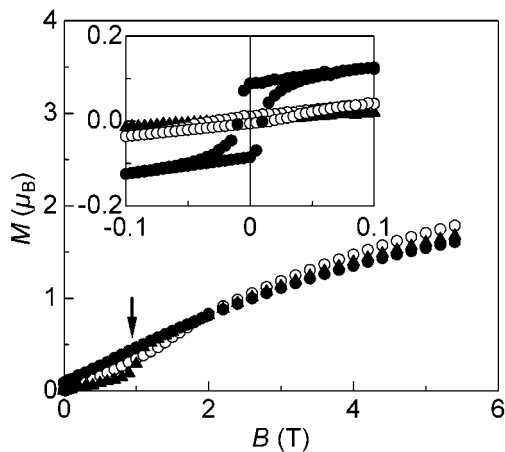


(b)

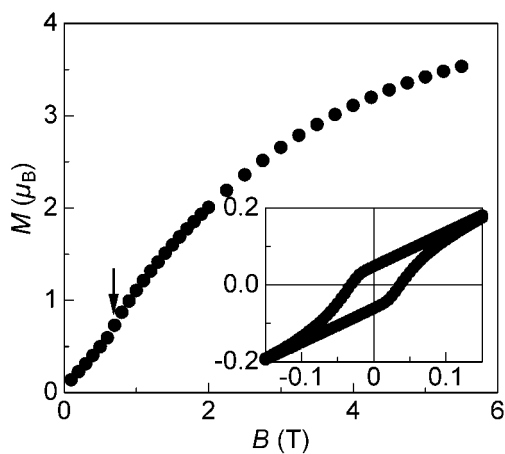
Figure 3. Temperature dependence of $\chi_M T$ (●) and χ_M^{-1} (○) for nonoriented samples, measured with an applied field of 10 mT for (a) compound **1** and (b) compound **2**. Solid lines are the Curie–Weiss law ($C = 2.19 \text{ emu K mol}^{-1}$, $\Theta = -20.4 \text{ K}$ for **1** and $C = 4.95 \text{ emu K mol}^{-1}$, $\Theta = -10.1 \text{ K}$ for **2**) fitted above 50 K. Insets: temperature dependence of the field-cooled magnetization (●) and remnant magnetization (○).

sured at 10 mT and the remnant magnetization (RM) observed after the external field of 10 mT is removed at 1.8 K. Below $T_C = 7.6 \text{ K}$ the FCMs steeply increase and the RMs also emerge, showing the presence of the spontaneous magnetization.

Figure 4 shows the magnetization curve at $T = 2 \text{ K}$ measured on oriented crystalline samples for **1** and on nonoriented microcrystalline samples for **2**. As the field increases, the magnetization tends to reach the value of $2\mu_B$ and $4\mu_B$ for **1** and **2**, respectively. These results correspond to all anion spins ($S = 3/2$ for **1**, $5/2$ for **2**) aligned in the field direction and all donor spins ($S = 1/2$) in the opposite direction; that is, a ferrimagnetic chain is realized for both salts. For compound **1**, a spin-flop transition is observed around $B = 1 \text{ T}$ (arrow in Figure 4a) when the external field B is parallel to the c -axis. When B is parallel to b , a hysteresis loop is observed, as shown in the inset of Figure 4a. The remanent magnetization and the coercive force in this direction are estimated as $M_r = 0.10 \mu_B$ and $B_c = 10 \text{ mT}$, respectively. The orthogonality of the spin-easy axis (c -axis)



(a)



(b)

Figure 4. Magnetization curves at 2 K for **1** measured on oriented samples (○: $B||a$, ●: $B||b$, and ▲: $B||c$), and for **2** measured on nonoriented samples. Arrows indicate the spin-flop transitions. Insets: hysteresis loop around $B = 0 \text{ T}$.

and the spontaneous magnetization direction (b -axis) clearly evidences the canted weak ferromagnetism. From the ratio of the remanent magnetization ($0.10 \mu_B$) to the magnetization at the high-field limit ($2\mu_B$), the spin-canting angle is estimated as $\sin^{-1}(0.10\mu_B/2\mu_B) = 2.9^\circ$, which is about one-third of the canting angle of the molecular axes for the two adjacent anions ($9.31(8)^\circ$). Although measurements on single crystalline samples cannot be performed for compound **2** as the samples are too small, its magnetic property can be discussed from analogy with compound **1**. On the magnetization curve a broad anomaly is observed at $B = 0.8 \text{ T}$ (arrow in Figure 4b), which can be assigned to a spin from transition. Moreover, a hysteresis loop is observed around $B = 0 \text{ T}$ also for this compound. Although the coercive force is difficult to estimate due to the random orientation, we can estimate the remanent magnetization of **2** from the hysteresis loop as $0.05/\cos\theta = 0.10 \mu_B$, where $\cos\theta = 1/2$ is the average of the direction cosine. The spin-canting angle is therefore estimated as $\sin^{-1}(0.10\mu_B/4\mu_B) = 1.4^\circ$, which is smaller than the corresponding value of the Cr salt.

The ESR spectra on microcrystalline samples of both compounds give single Lorentzian signals in the whole

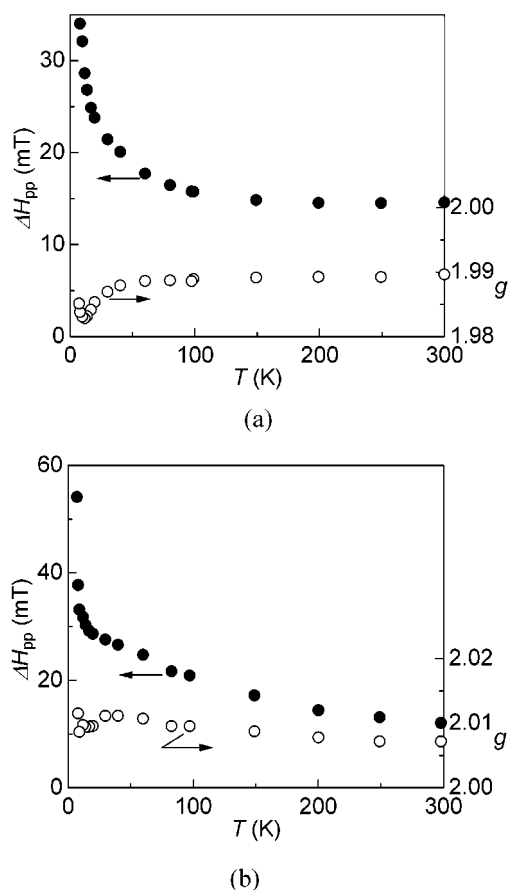


Figure 5. Temperature dependence of the ESR g -value (○) and peak-to-peak line width ΔH_{pp} (●) for (a) compound **1** and (b) compound **2**.

temperature range without separating the donor and anion spins, suggesting the presence of an exchange interaction between these two spin species. Figure 5 shows the temperature dependence of the g -value and the peak-to-peak line width. The g -value of compound **1** at room temperature (1.989) is close to the value of $\text{K}_3[\text{Cr}(\text{CN})_6]$ (1.992),¹³ showing that the observed ESR signal mainly comes from the Cr^{3+} spins. For compound **2**, the g -value of the ESR absorption (2.007) is closer to the free-electron value (2.0023) than $\text{K}_3[\text{Fe}(\text{CN})_6]$ ($g_x = 2.35$, $g_y = 2.10$, $g_z = 0.91$),¹³ which also supports the coalescence of the donor and anion spins. The line widths at room temperature are 14.6 and 12.1 mT for **1** and **2**, respectively. These values are smaller than the corresponding dipolar widths 35 mT (**1**) and 57 mT (**2**) (calculated for $S = 3/2$ or $5/2$ anion spins and $S = 1/2$ donor spins and averaged for all directions), showing the effect of the exchange narrowing. For compound **1**, as the temperature decreases down to ca. 60 K, the g -value gradually decreases, and then it decreases steeply down to 1.983 at 12 K. This g -value shift suggests the presence of spin fluctuation above the magnetic transition temperature, caused by the one-dimensional nature of the ferrimagnetic chain. The line width increases gradually as the temperature decreases below 100 K and shows a divergence as a precursor of a magnetically ordered state, which is featured with the canted weak

ferrimagnet as suggested by the magnetization measurements. For compound **2**, on the other hand, the g -value has a smaller temperature dependency than compound **1**. A possible explanation is that Fe^{3+} has a larger spin quantum number ($S = 5/2$) than Cr^{3+} ($S = 3/2$); hence the quantum nature of the localized spins are diminished to suppress the spin fluctuation.

The spin structure in the magnetically ordered phase can be discussed from the crystal structure. The short $\text{S}\cdots\text{S}$ contacts between the thiocyanate ligands of the anion and the tetrathiapentalene ring of the donor realize the intrachain antiferromagnetic interaction between the anion ($S = 3/2$ or $5/2$) and donor ($S = 1/2$) spins, resulting in the ferrimagnetic structure within the chain. On the other side, the adjacent anions are also connected via the π -overlap of isoquinoline ligands, which can be an interchain exchange path between the anion spins. The distorted MN_6 coordination octahedra have an axial D_{4h} symmetry, which leads to the single-ion anisotropy of the anion complex. Furthermore, the two adjacent anions are not related by inversion symmetry. Therefore the origin of the weak ferromagnetic interaction between the ferrimagnetic chains can be ascribed to the canting of the magnetic anisotropy axes of adjacent anions and/or the presence of the Dzyaloshinsky–Moriya interaction¹⁴ between the adjacent magnetic anions.

Conclusion

Two new charge transfer salts $(\text{BDH-TTP})\text{M}(\text{isoq})_2(\text{NCS})_4$ with $\text{M} = \text{Cr}^{\text{III}}$ (**1**) and Fe^{III} (**2**) made of a non-TTF donor and metal complex anions were prepared and structurally and magnetically characterized. These two compounds are isostructural to each other with 1:1 stoichiometry. The crystal structure contains mixed chains of organic and inorganic units with alternate anion ($S = 3/2$ and $S = 5/2$ for **1** and **2**, respectively) and donor ($S = 1/2$) spins. These salts undergo a bulk weak ferromagnetic state originating from the canted alignment of the one-dimensional ferrimagnetic chains involving d electrons and π electrons. The origin of the intrachain antiferromagnetic coupling is the short intermolecular $\text{S}\cdots\text{S}$ contacts between donors and anions, whereas the interchain coupling comes from the π - π overlapping between anions and/or $\text{S}\cdots\text{S}$ contacts between donors. The richness of this series of molecular materials in terms of synthetic chemistry and physical properties opens a wide range of perspectives.

Acknowledgment. We are grateful for the financial support from the CNRS, CNRS-JSPS PICS program No 1433 and NEDO research project 00MB4, and a Grant-in-Aid for Scientific Research on Priority Area (No. 12046231) from the Ministry of Education, Science, Sports, and Culture, Japan. F.S. thanks the French and Algerian Ministries of Education for a Ph.D. fellowship.

Supporting Information Available: X-ray crystallographic files, in CIF format, are available free of charge via the Internet at <http://pubs.acs.org>.

IC025553K

(13) Baker, J. M.; Bleaney, B.; Bowers, K. D. *Proc. Phys. Soc.* **1956**, *B69*, 1205.

(14) (a) Dzyaloshinski, I. *J. Phys. Chem. Solids* **1958**, *4*, 241. (b) Moriya, T. *Phys. Rev.* **1960**, *120*, 91.